Journal of Zhejiang University SCIENCE A
ISSN 1673-565X (Print); ISSN 1862-1775 (Online)
www.zju.edu.cn/jzus; www.springerlink.com
E-mail: jzus@zju.edu.cn

Parameters optimization and nonlinearity analysis of grating eddy current displacement sensor using neural network and genetic algorithm

Hong-li QI[1,2], Hui ZHAO[†‡1], Wei-wen LIU[1], Hai-bo ZHANG[1]

([1]*Department of Instrument Science and Engineering, Shanghai Jiao Tong University, Shanghai 200240, China*)

([2]*Instrumentation Science and Dynamic Measurement Laboratory, North University of China, Taiyuan 030051, China*)

[†]E-mail: huizhao@sjtu.edu.cn

Received July 25, 2008; Revision accepted Mar. 5, 2009; Crosschecked May 27, 2009

Abstract: A grating eddy current displacement sensor (GECDS) can be used in a watertight electronic transducer to realize long range displacement or position measurement with high accuracy in difficult industry conditions. The parameters optimization of the sensor is essential for economic and efficient production. This paper proposes a method to combine an artificial neural network (ANN) and a genetic algorithm (GA) for the sensor parameters optimization. A neural network model is developed to map the complex relationship between design parameters and the nonlinearity error of the GECDS, and then a GA is used in the optimization process to determine the design parameter values, resulting in a desired minimal nonlinearity error of about 0.11%. The calculated nonlinearity error is 0.25%. These results show that the proposed method performs well for the parameters optimization of the GECDS.

Key words: Grating eddy current displacement sensor (GECDS), Artificial neural network (ANN), Genetic algorithm (GA), Parameters optimization, Nonlinearity error

doi:10.1631/jzus.A0820564 **Document code:** A **CLC number:** TH7; TM15

INTRODUCTION

In order to solve the contradiction between long range and high accuracy in displacement or position measurement, a grating structure has been used in many sensors, such as optical sensors, capacitive sensors, magnetic sensors and inductive sensors (Mitutoyo Corporation, 1998; Hall *et al*., 2002; Davidenko and Al-Kadhimi, 2004; Prelle *et al*., 2006). Among these sensors, the grating optical sensor and grating capacitive sensor are sensitive to contaminations caused by water, oil and other fluids, and the grating magnetic sensor is easily affected by ferromagnetic particles. So these sensors must be sealed or encapsulated to restrain contaminations from diminishing their effectiveness in difficult industry conditions. Compared to the above mentioned three kinds of sensors, the grating inductive sensor is insensitive not only to contaminations caused by fluids and dust, but also to ferromagnetic particles. Thus, the grating inductive sensor has been widely used in watertight electronic transducers (Mitutoyo Corporation, 1998; 2002). However, the exciting coil and pickup coil of the grating inductive sensor are detached and the shape of the pickup coil is relatively complex, which will increase manufacturing and assembly costs of the sensor.

In this paper we introduce a grating displacement sensor based on the eddy current effect proposed in (Zhao *et al*., 2004a; 2004b). The grating eddy current displacement sensor (GECDS) exhibits the characteristic of being resistant to liquid, dust and ferromagnetic particles when used as an inductive sensor in watertight electronic transducers to realize

‡ Corresponding author

long range displacement or position measurement with high accuracy in difficult industry conditions. Different from the sensor structure presented in most previous literature that uses two coils for the functions of excitation and picking up signals (Kacprzak *et al*., 2001; Yamada *et al*., 2004; Dinulovic and Gatzen, 2006), this sensor structure uses the same coil for both functions.

To improve the sensor's characteristics, we should first know the influence of the design parameters. Due to complexity of structure and the 3D eddy current field of the GECDS, an analytic model is too difficult to use, so the optimization design of the sensor has been a challenging task. Computer aided design has made a major impact on parameters optimization for both quality improvement and cost reduction in the manufacturing process based on applications of various computer simulation techniques. The influence of parameters on inductance variation of the GECDS coils has been studied by means of electromagnetic fields modeling software (Zhou *et al*., 2005), which lacks accuracy and needs substantial computation time. Other characteristics of the GECDS have not been studied till now. Measurement accuracy of the sensor is affected by inherent systematic errors, such as the nonlinearity of the system (Zhang and Kiyono, 2001). For the GECDS, nonlinearity is caused not only by the eddy current effect, but also by the mechanical and electrical design and assembly process. The main objective of this study is to investigate the influence of design parameters on the nonlinearity of the GECDS, and to realize multi-parameter optimization to improve the sensor quality.

Advanced methods are expected for modeling and optimizing the GECDS for the purpose of manufacturing high quality sensors. In recent years, the artificial neural network (ANN) has become a very useful method for modeling very complex nonlinear systems, and the genetic algorithm (GA) as an efficient search algorithm is widely used in many research areas for parameter optimization (Cook *et al*., 2000; Shen *et al*., 2007). These two methods are considered to be feasible in multi-parameter optimization of the GECDS due to their complexity.

This study combines the ANN and GA to investigate the relationship between design parameters and the nonlinearity error of the GECDS. The proposed method tries to take advantage of the prediction accuracy of ANN and the efficiency of GA in optimizing design parameters. First, we set up a neural network model to predict the nonlinearity error of the GECDS. Then a GA is used to determine the optimal design parameters of the sensor, which would result in a better output signal exhibiting an improved linearity. The optimized results match the simulation results well. Finally, this technique is integrated with electromagnetic field simulation software Maxwell™ to minimize the time and cost for the efficient design of the GECDS.

GECDS

Fig.1 shows the schematic diagram of the GECDS. The measurement principle of this sensor has been described in our previous work (Qi *et al*., 2009). When an alternating current with a high frequency passes through the coil (which moves transversely), the inductance of the coil varies periodically.

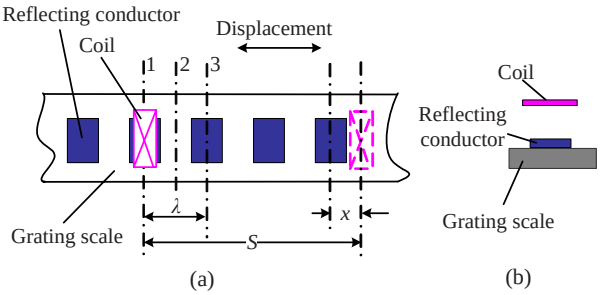

Fig.1 Schematic diagram of the GECDS
(a) Front view; (b) Side view

The displacement between the coil and reflectors, *S*, could be converted into inductance variation of the coil. The displacement *S* can be calculated by

$$S=n\lambda+x, \tag{1}$$

where *S* is the displacement between the coil and reflecting conductors, *n* is the number of complete cycles, and *x* is the small displacement in one cycle λ.

To enhance measurement sensitivity and to avoid measurement blind areas, an arrangement with four coils is used. Fig.2 shows the schematic representation of the arrangement.

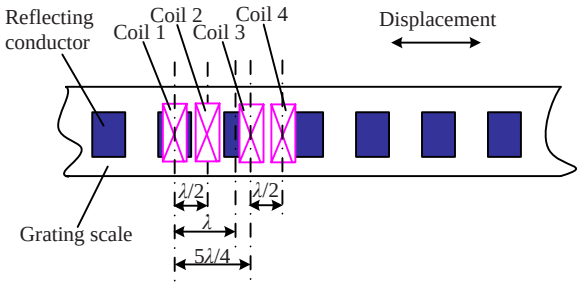

Fig.2 Schematic diagram of the arrangement with four coils

Coils 1 and 2 output differential frequency signal $f_{12}=f_1-f_2$ and coils 3 and 4 output differential frequency signal $f_{34}=f_3-f_4$. Since coils 1 and 2 and coils 3 and 4 are apart from each other by $5\lambda/4$, waveforms of differential frequency against displacement are shifted in phase for $\lambda/4$. The differential frequencies are shown in Fig.3.

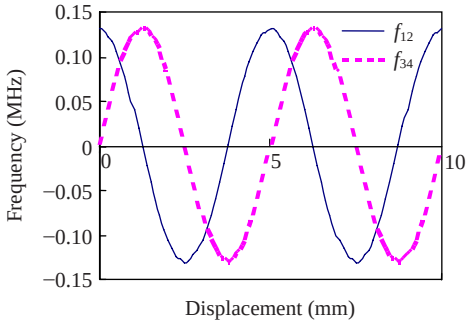

Fig.3 Differential frequency waveforms

Because the differential frequency curve f_{12} draws close to the cosine curve and the differential frequency curve f_{34} draws close to the sinusoidal curve, curves f_{12} and f_{34} can be roughly expressed as follows:

$$f_{12} = A\cos(2\pi x / \lambda), \quad (2)$$

$$f_{34} = A\sin(2\pi x / \lambda). \quad (3)$$

Let the phase angle be

$$\varphi = 2\pi x / \lambda. \quad (4)$$

Then

$$\varphi = \arctan\left(\frac{f_{34}}{f_{12}}\right) = \arctan\left[\frac{\sin(2\pi x / \lambda)}{\cos(2\pi x / \lambda)}\right]. \quad (5)$$

Fig.4 illustrates the linear phase angle changes vs. the displacement which is equal to the length of two cycles according to Eq.(5). It can be seen that the phase angle φ is proportional to the displacement in a complete cycle, so the small displacement x can be obtained through phase angle φ:

$$x = \lambda\varphi / (2\pi). \quad (6)$$

Assuming n (the number of cycles) has been acquired, the displacement S can be calculated by Eq.(1).

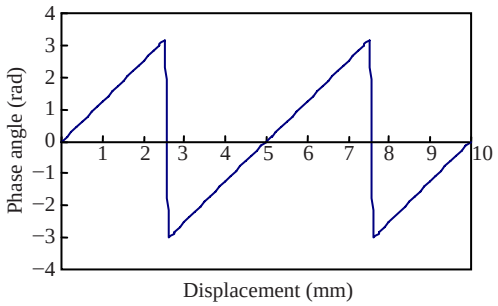

Fig.4 Linear phase angle changes vs. displacement

SIMULATIOIN MODEL

Due to the highest inductance density of the spiral coil configuration compared to the planar coil (Hamasaki and Ide, 1995), multi-layer planar rectangular spiral coils have been selected for our work (Qi *et al.*, 2009). The sensor model with multi-layer coils is presented in Fig.5, where the structure is simplified to a stack of only 2-layer planar spiral coils. The parameters of the sensor model are defined as follows: a, length of the reflecting conductor; b, width of the reflecting conductor; D_1, length of the coil; D_2, width of the coil; d_1 and d_2, inner diameters of the coil; c_1, thickness of the single-layer coil; c_2, thickness of the reflecting conductor; h, axial gap between the coil and reflecting conductor; s, width of the copper traces; t, the gap between copper traces; n, number of turns per layer; f, excitation frequency. In this study we set c_1=0.03 mm, c_2=0.06 mm, s=t=0.1 mm, n=4, and f=3 MHz.

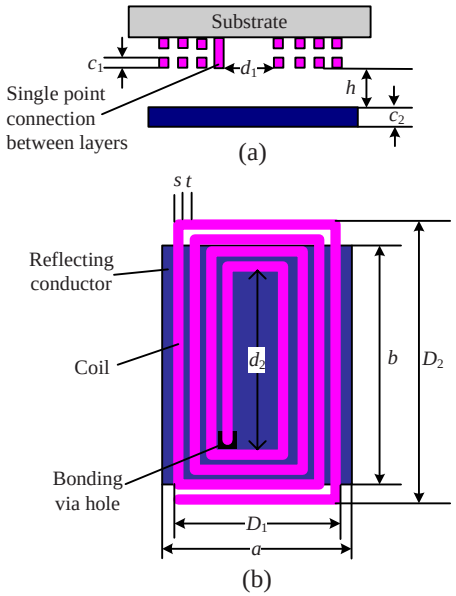

Fig.5 Schematic presentation of multi-layer coils
(a) Front view; (b) Plan view

NONLINEARITY ERROR ANALYSIS OF GECDS

It is worth noting that the linear relationship between the phase angle and displacement in one complete cycle is obtained based on the assumption that differential frequency curves are ideal sinusoidal and cosine curves. In fact, this relationship is nonlinear due to the nonlinearity of the eddy current effect and systematic errors in the manufacturing and assembly processes.

The nonlinearity error of the GECDS can be expressed in a percentage ratio of the maximum deviation of the measured phase angle from the idealized straight line (Fig.4) to the span of phase angle variation over the fixed cycle λ, i.e.,

$$E=\frac{\left|\varphi_{\mathrm{m}}-\varphi_{\mathrm{i}}\right|_{\max}}{2\pi}\times 100\%\,, \tag{7}$$

where E is the nonlinearity error of the GECDS, φ_{m} is the measured phase, and φ_{i} is the idealized phase angle.

The main objective of this paper is to investigate the influence of design parameters on the nonlinearity of the GECDS. The GECDS has many design parameters, as shown in Fig.5. It would be very complicated if we consider all design parameters in simulation. Since geometric parameters of spiral coils are more complex than those of a reflecting conductor, simulations are performed through changing the parameters of a reflecting conductor and axial gap. At given values of other parameters, the parameters that affect the nonlinearity error are: the length of the reflecting conductor (*a*), the width of the reflecting conductor (*b*), and the axial gap between the coil and reflecting conductor (*h*). Here the thickness of the reflecting conductor is 0.06 mm, which is larger than the penetration depth of the eddy current. Due to the electric current of the coils being very small, the temperature effect coming from eddy current self-heating effect is disregarded.

We can obtain the nonlinearity errors of different sets of parameters through electromagnetic field simulation. We use 3D response surface plots to graphically illustrate variation trends in the nonlinearity error. The effects of altering design parameters *a*, *b* and *h* for nonlinearity are shown in Figs.6~8.

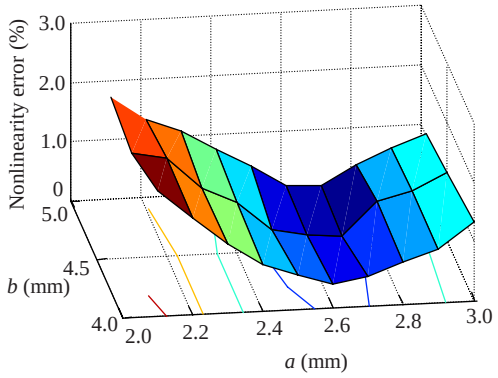

Fig.6 Effect of *a* and *b* on nonlinearity with *h*=0.5 mm
a and *b* are the length and width of the reflecting conductor, respectively; *h* is the axial gap between the coil and reflecting conductor

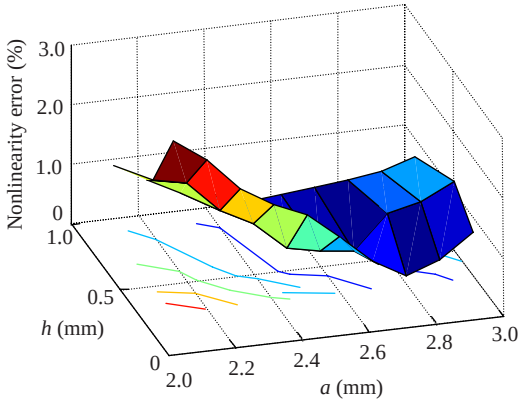

Fig.7 Effect of *a* and *h* on nonlinearity with *b*=4.5 mm
a and *b* are the length and width of the reflecting conductor, respectively; *h* is the axial gap between the coil and reflecting conductor

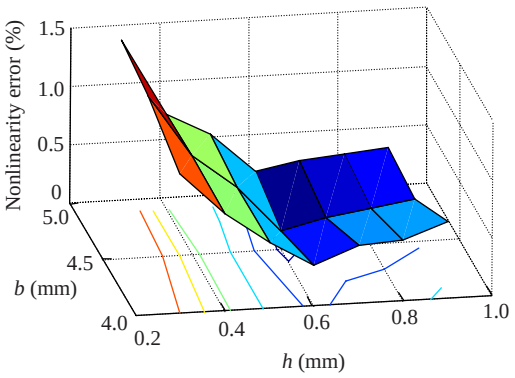

Fig.8 Effect of *h* and *b* on nonlinearity with *a*=2.5 mm
a and *b* are the length and width of the reflecting conductor, respectively; *h* is the axial gap between the coil and reflecting conductor

Fig.6 shows the change in the nonlinearity error in terms of *a* and *b* with *h*=0.5 mm. Fig.7 shows the change in the nonlinearity error in terms of *a* and *h* with *b*=4.5 mm. Fig.8 shows the change in the nonlinearity error in terms of *b* and *h* with *a*=2.5 mm. Figs.6 and 7 both show that the nonlinearity error decreases first and then increases when the length of the reflecting conductor changes from 2.1 to 3.0 mm. Fig.8 shows that the nonlinearity error decreases first and then increases slowly when the axial gap changes from 0.3 to 0.9 mm. Figs.6 and 8 show that the variation in the nonlinearity error is not obvious when the reflecting conductor width is changed. These three figures show that there is a nonlinear relationship between the three design parameters and the nonlinearity error. Because the three graphics are all approximately concave, the nonlinearity error would have a minimum value at some points on the surface plots.

PARAMETER OPTIMIZATION

The above nonlinearity analysis using an exhaustive algorithm reveals the variation in the nonlinearity error when altering parameter values, but it cannot determine the parameter values that would result in a desired minimal nonlinearity error. So we need to investigate a method to optimize design parameters of the GECDS. A method combining ANN and GA is proposed to optimize the design parameters of the sensor in this study.

The connection of ANN, GA and electromagnetic simulation is shown in Fig.9. We use the electromagnetic field simulation software Maxwell™ to compute the nonlinearity errors of different sets of design parameters. Design parameters and the nonlinearity error are both used as training samples of ANN to train the neural network. This neural network can build the relationship between design parameters and the nonlinearity error through learning. The trained network can be used to predict the nonlinearity error of the design parameters, which are different from those of training samples. Then, GA is used to optimize the design parameters to obtain the minimal nonlinearity error. In the optimization process, the trained neural network is used to calculate the fitness (nonlinearity error) of the objective function. In the implementation we use MATLAB to develop the program of the optimization algorithm.

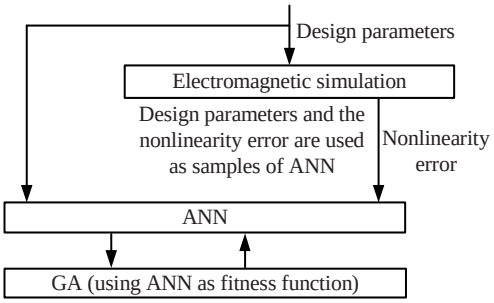

Fig.9 Connection of artificial neural network (ANN), genetic algorithm (GA) and electromagnetic simulation

Design of the ANN model of the GECDS

ANN has a significant nonlinear mapping capability to learn an arbitrary nonlinear relationship between input and output parameters, which has been widely applied in industrial applications to simulate complex problems and to predict parameter values of the manufacturing process (Pratap *et al*., 2004; Yang *et al*., 2006). Due to the complexity of the GECDS, it is a difficult task to build the relationships between design parameters and the nonlinearity error expressed by any analytical model. The characteristics of ANN make it suitable for modeling the output parameters prediction of the GECDS, so it is used in this work.

Back propagation network (BPN) is a typical ANN (Shen *et al*., 2007). A three-layer BPN is used in this study. The GECDS has three design parameters as the inputs of the BPN, and one output parameter, as

well as the nonlinearity error as the output of the BPN. Thus, the full BPN consists of three input nodes and one output node, as shown in Table 1. The node numbers of the input, output and hidden layers are determined by the numbers of design parameters, output parameters and trials, respectively. The network structure is adjusted by changing the node number in the hidden layer. The network structure is optimized to obtain the minimal modeling error measured by mean-square-error (MSE). $|\Delta E|_{\max}$ is the maximum deviation of the predicted nonlinearity error from the simulation value. Based on the comparison of the three structures shown in Table 1, we select the 3-38-1 network structure, which has the minimal modeling error $4.611\,43\times10^{-7}$ and $|\Delta E|_{\max}$ is 0.20%.

Table 1 Optimized neural network parameters

BPN structure*	Training MSE	$\|\Delta E\|_{\max}$ (%)
3-38-1	4.611 43E−7	0.20
3-25-1	5.846 92E−7	0.20
3-29-1	7.600 93E−7	0.42

* In the *x*-*y*-*z* structure, *x*, *y*, and *z* refer to the number of input, hidden, and output layers, respectively

In this work, an electromagnetic field simulation computer is used to obtain nonlinearity errors of different sets of parameters. The samples of the BPN are composed of design parameters and the nonlinearity error. Fig.10a shows the trained results with 44 training samples. We can see that the trained values have good consistency with the simulative values. Thus, this trained network can map the complicated nonlinearity relationship between design parameters and the nonlinearity error. Another 16 samples are used to test the prediction performance of this network. As shown in Fig.10b, the predicted nonlinearity errors of most of the testing samples are consistent with the simulative values. The maximum deviation of the predicted nonlinearity error from the simulative value $|\Delta E|_{\max}$ is 0.20%. The results demonstrate that the network has better prediction performance.

Parameters optimization using GA

GA is a powerful tool for global search and optimization. It can solve nonlinear problems by searching all spaces through selection, crossover, and mutation operations to obtain a set of desired design parameters (Pratap *et al*., 2004; Shen *et al*., 2007).

GA starts with a randomized initial population of parent chromosomes, and then causes the parent population to evolve to a population which is expected to have a better solution for some problems. In general GA operates through the following two steps: (1) Chromosomes of the current population are selected with a given probability. The selection of chromosomes is based on an objective function and the fittest will survive into the next generation. (2) New offspring chromosomes are created by crossover and mutation. The crossover recombines information from two good parents and passes it on to offspring. The mutation can introduce innovation into the population. The population of the next generation has a better fitness globally (Cook *et al*., 2000; Yang *et al*., 2006; Shen *et al*., 2007).

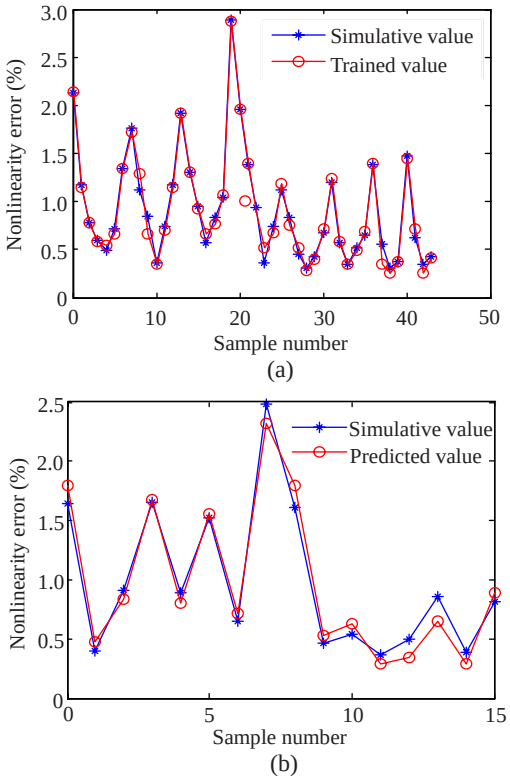

Fig.10 (a) Trained results with 44 training samples; (b) Test results with another 16 samples

A chromosome is made up of genes. The gene within a chromosome, namely the individual in the population, is considered as an input parameter in application. A chromosome can be represented by a sequence of binary digits. The value of the binary digit is within the upper and lower bounds of the design parameter. The three design parameters are

used to represent the genes within chromosomes and each chromosome is composed of three genes. The selection is based on the individual's fitness function. The trained BPN is used to evaluate an individual's fitness. The single-point crossover and discrete mutation are used.

The three design parameters are set as follows: a=2.1~3.0 mm, b=4.0~4.9 mm, and h=0.3~0.9 mm. The design parameters are optimized by GA. The population size is set to 20 and the maximum number of generations is 30. The trained BPN is used as an objective function to calculate the nonlinearity error of different sets of parameters. The process of optimization is shown in Fig.11. The optimized results are set as follows: a=2.4857 mm, b=4.7714 mm, h=0.6429 mm, and the minimal nonlinearity error is approximately 0.11%. The minimal nonlinearity error is smaller than the nonlinearity errors of all training and testing samples. Thus the optimization result is satisfying.

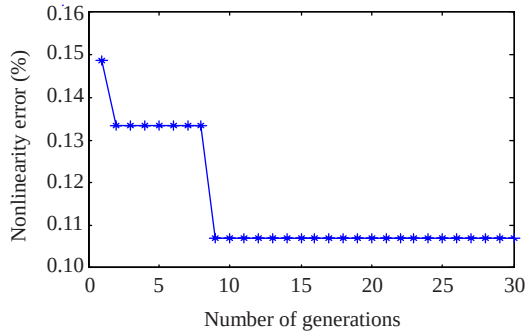

Fig.11 Evolution of generation for optimization

Verification of the optimization result

The electromagnetic field simulation has been conducted in terms of the optimized design parameters a=2.4857 mm, b=4.7714 mm, and h=0.6429 mm. The calculated nonlinearity error is 0.25%, which is larger than the optimization result of about 0.11%, but smaller than the nonlinearity errors of all training and testing samples. The results demonstrate that we can obtain the minimal nonlinearity error with the optimized design parameters. The difference between the optimized and simulation results is caused mainly by the prediction error of BPN. The functional mapping representative of the testing samples should be as accurate as that of the training samples. If the functional mapping of the BPN has higher prediction accuracy, this problem would be well solved.

CONCLUSION

The method of combining ANN and GA for design parameters optimization has been developed for the GECDS. A BPN is set up to predict the nonlinearity error of the sensor. GA is then applied, using the network to evaluate fitness, to determine which set of design parameters would result in the desired minimal nonlinearity error. The optimal design parameter values are obtained.

The combination of ANN and GA can be used as a promising method for studying the complicated relationship between design parameters and output characteristics of a sophisticated system. This technique can also provide designers and manufacturers with useful information that will help them to adjust parameters in time. There are some constraints in application, however, such as the configuration of the design parameters and the prediction accuracy of the ANN model. The Taguchi method and response surface method may be better methods integrated with GA.

References

Cook, D.F., Ragsdalt, C.T., Major, R.L., 2000. Combining a neural network with a genetic algorithm for process parameter optimization. *Eng. Appl. Artif. Intell.*, **13**(4): 391-396. [doi:10.1016/S0952-1976(00)00021-X]

Davidenko, I.I., Al-Kadhimi, A.J., 2004. Magnetic grating in garnets in spatially periodic effective and real magnetic field. *J. Magn. Magn. Mater.*, **272-276**:363-364. [doi:10.1016/j.jmmm.2003.11.135]

Dinulovic, D., Gatzen, H.H., 2006. Microfabricated inductive micropositioning sensor for measurement of a linear movement. *IEEE Sens. J.*, **6**(6):1482-1487. [doi:10.1109/JSEN.2006.884439]

Hall, N.A., Lee, W., Dervan, J., Degertekin, F.L., 2002. Micromachined Capacitive Transducer with Improved Optical Detection for Ultrasound Applications in Air. IEEE Ultrasonics Symp., p.1027-1030.

Hamasaki, Y., Ide, T., 1995. Fabrication of Multi-layer Eddy Current Micro Sensors for Non-destructive Inspection of Small Diameter Pipes. Proc. IEEE Micro Electro Mechanical Systems, p.232-237. [doi:10.1109/MEMSYS.1995.472574]

Kacprzak, D., Taniguchi, T., Nakamura, K., Yamada, S., Iwahara, M., 2001. Novel eddy current testing sensor for the inspection of printed circuit boards. *IEEE Trans. Magn.*, **37**(4):2010-2012. [doi:10.1109/20.951037]

Mitutoyo Corporation, 1998. Induced Current Absolute Position Transducer Using a Code-track-type Scale and Read Head. US Patent, 08/790 494.

Mitutoyo Corporation, 2002. Electronic Caliper Using a Reduced Offset Induced Current Position Transducer. US Patent, 09/527 518.

Pratap, R.J., Sarkaf, S., Pinel, S., Laskar, J., May, G.S., 2004. Modeling and Optimization of Multilayer LTCC Inductors for RF/Wireless Application Using Neural Network and Genetic Algorithms. IEEE Electronic Components and Technology Conf., p.248-254.

Prelle, C., Lamarque, F., Revel, P., 2006. Reflective optical sensor for long-range and high-resolution displacements. *Sens. Actuat. A*, **127**(1):139-146. [doi:10.1016/j.sna.2005.11.005]

Qi, H.L., Zhao, H., Liu, W.W., 2009. Characteristics analysis and parameters optimization for the grating eddy current displacement sensor. *J. Zhejiang Univ. Sci. A*, **10**(7):1029-1037. [doi:10.1631/jzus.A0820358]

Shen, C.Y., Wang, L.X., Li, Q., 2007. Optimization of injection molding process parameters using combination of artificial neural network and genetic algorithm method. *J. Mater. Process. Technol.*, **183**(2-3):412-418. [doi:10.1016/j.jmatprotec.2006.10.036]

Yamada, S., Chomsuwan, K., Fukuda, Y., Iwahara, M., Wakiwaka, H., Shoji, S., 2004. Eddy-current testing probe with spin-valve type GMR sensor for printed circuit board inspection. *IEEE Trans. Magn.*, **40**(4): 2676-2678. [doi:10.1109/TMAG.2004.829254]

Yang, T., Lin, H.C., Chen, M.L., 2006. Metamodeling approach in solving the machine parameters optimization problem using neural network and genetic algorithms: a case study. *Rob. Comput.-Integr. Manuf.*, **22**(4):322-331. [doi:10.1016/j.rcim.2005.07004]

Zhang, S.Z., Kiyono, S., 2001. An absolute calibration method for displacement sensors. *Measurement*, **29**(1):11-20. [doi:10.1016/S0263-2241(00)00023-3]

Zhao, H., Ma, D.L., Liu, W.W., Yu, P., 2004a. Design of a new inductive grating displacement sensor and application in liquid resistant caliper. *J. Shanghai Jiao Tong Univ.*, **38**(8):1382-1384 (in Chinese).

Zhao, H., Liu, W.W., Yu, P., Tao, W., 2004b. Summary on water-proof electronic digital caliper. *New Technol. New Process*, (12):7-10. (in Chinese).

Zhou, D.L., Zhao, H., Liu, W.W., Hong, H.T., 2005. 3-D FEA simulating study on the parameters of eddy current displacement sensor. *Comput. Meas. Control*, **13**(6):618-620 (in Chinese).